Broad-spectrum non-nucleoside inhibitors for caliciviruses

Natalie E. Netzler [a], Daniel Enosi Tuipulotu [a,] Auda A. Eltahla [a,b], Jennifer H. Lun[a], Salvatore Ferla [c], Andrea Brancale [c], Nadya Urakova [d,e,f], Michael Frese [d,e,f,g], Tanja Strive [d,f,g], Jason M. Mackenzie [h,i] and Peter A. White [a#].

[a] *School of Biotechnology and Biomolecular Sciences, University of New South Wales, Sydney, NSW, Australia*

[b] *School of Medical Sciences, Faculty of Medicine, University of New South Wales, Sydney, NSW, Australia*

[c] *School of Pharmacy and Pharmaceutical Sciences, Cardiff University, Cardiff, United Kingdom*

[d] *CSIRO Health and Biosecurity, Canberra, ACT, Australia*

[e] *Invasive Animals Cooperative Research Centre, University of Canberra, ACT, Australia*

[f] *Health Research Institute, University of Canberra, ACT, Australia*

[g] *Institute for Applied Ecology, University of Canberra, ACT, Australia*

[h] *Department of Microbiology and Immunology, School of Biomedical Sciences, University of Melbourne, VIC, Australia*

[i] *The Peter Doherty Institute for Infection and Immunity, VIC, Australia.*

Running head: Broad-spectrum non-nucleoside polymerase target sites

[#] Corresponding author at: School of Biotechnology and Biomolecular Sciences, University of New South Wales, Sydney, NSW, Australia. Tel.: +61 9385 3780.

E-mail address: p.white@unsw.edu.au (P.A. White).

Abstract

Viruses of the *Caliciviridae* cause significant and sometimes lethal diseases, however despite substantial research efforts, specific antivirals are lacking. Broad-spectrum antivirals could combat multiple viral pathogens, offering a rapid solution when no therapies exist. The RNA-dependent RNA polymerase (RdRp) is an attractive antiviral target as it is essential for viral replication and lacks mammalian homologs. To focus the search for pan-*Caliciviridae* antivirals, the RdRp was probed with non-nucleoside inhibitors (NNIs) developed against hepatitis C virus (HCV) to reveal both allosteric ligands for structure-activity relationship enhancement, and highly-conserved RdRp pockets for antiviral targeting. The ability of HCV NNIs to inhibit calicivirus RdRp activities was assessed using *in vitro* enzyme and murine norovirus cell culture assays. Results revealed that three NNIs which bound the HCV RdRp Thumb I (TI) site also inhibited transcriptional activities of six RdRps spanning the *Norovirus*, *Sapovirus* and *Lagovirus* genera of the *Caliciviridae*. These NNIs included JTK-109 (RdRp inhibition range: IC_{50} 4.3–16.6 μM), TMC-647055 (IC_{50} range: 18.8–45.4 μM) and Beclabuvir (IC_{50} range: 23.8–>100 μM). *In silico* studies and site-directed mutagenesis indicated the JTK-109 binding site was within the calicivirus RdRp thumb domain, in a pocket termed Site-B, which is highly-conserved within all calicivirus RdRps. Additionally, RdRp inhibition assays revealed that JTK-109 was antagonistic with the previously reported RdRp inhibitor pyridoxal-5'-phosphate-6-(2'-naphthylazo-6'-nitro-4',8'-disulfonate) tetrasodium salt (PPNDS), that also binds to Site-B. Moreover, like JTK-109, PPNDS was also a potent inhibitor of polymerases from six viruses spanning the three *Caliciviridae* genera tested (IC_{50} range: 0.1–2.3 μM). Together, this study demonstrates the potential for *de novo* development of broad-spectrum antivirals that target the highly-conserved RdRp thumb pocket, Site-B. We also revealed three

broad-spectrum HCV NNIs that could be used as antiviral scaffolds for further development against caliciviruses and other viruses.

Key words

Broad-spectrum antivirals; non-nucleoside inhibitors; direct-acting antivirals; norovirus; RNA-dependent RNA polymerase; *Caliciviridae*

Abbreviations

BS-AV, broad-spectrum antivirals; CI, confidence intervals; FCV, feline calicivirus; IC_{50}, half maximal inhibitory concentration; HBV, hepatitis B virus; HCV, hepatitis C virus; HIV, human immunodeficiency virus; MNV, murine norovirus; NA, nucleoside analogue; NAF2, naphthalene di-sulfonate; NoV, norovirus; NNI, non-nucleoside inhibitor; NTP, nucleoside triphosphate; Pβ, Palm β; PDB, Protein Data Bank; PI, Palm I; PII, Palm II; PFU, plaque forming units; PPNDS, pyridoxal-5'-phosphate-6-(2'-naphthylazo-6'-nitro-4',8'-disulfonate) tetrasodium salt; RCV, rabbit calicivirus; RdRp, RNA-dependent RNA polymerase; RHDV, rabbit hemorrhagic disease virus; SaV, sapovirus; TI, Thumb I; TII, Thumb II.

1 Introduction

There is currently a lack of both narrow and broad-spectrum antivirals (BS-AVs) available to combat viral pathogens (1). This deficiency of BS-AVs is due to the complexity of viral replication strategies and their various host tropisms (2). Antivirals are generally targeted against a single viral species, for example: hepatitis B virus (HBV), hepatitis C virus (HCV), herpesviruses or human immunodeficiency virus (HIV) (3-5), and cross-species antiviral activity is rare. BS-AVs could be used to combat several clinically significant and emerging viral pathogens when no specific therapies exist (1). Additionally, they could be used as prophylaxis in an outbreak setting, to treat chronically infected patients, or when rapid and accurate diagnoses are not feasible (6). Given the global health burden created by caliciviruses, there is a necessity to develop safe and effective BS-AVs against all *Caliciviridae* pathogens.

One strategy in BS-AV development is to target conserved domains of viral enzymes critical for replication (1). The viral RNA-dependent RNA polymerase (RdRp) is an attractive antiviral target, given its highly-conserved structure across viral families. RdRps are essential for viral replication and largely lack host homologs, minimizing chances of off-target effects (7). Despite significant sequence diversity, all RdRps form structural homomorphs resembling a closed right-hand with fingers, palm and thumb domains (8, 9). To identify broadly conserved RdRp regions for further antiviral targeting, bioactive molecules can be identified by screening compounds or libraries using polymerase assays with RdRps from several viral species (10). This approach can reveal both highly-conserved viral enzyme domains, and BS-AV candidates with activity against different species, genera and families.

Caliciviruses are a diverse family of positive-sense RNA viruses, currently classified into five genera; *Norovirus, Sapovirus, Lagovirus*, *Nebovirus* and *Vesivirus* (11). Viruses from the

Caliciviridae cause significant diseases in a wide range of vertebrate hosts (12), and the substantial impact caused by caliciviruses is often underestimated (13-15). Currently there are no specific antivirals available for the treatment of calicivirus infections, and vaccines are only available for two viruses, feline calicivirus (FCV) and rabbit hemorrhagic disease virus (RHDV) (16, 17).

Among the caliciviruses that infect humans, norovirus (NoV) is a leading cause of acute gastroenteritis (18, 19), accounting for approximately 219,000 deaths annually (20). Antiviral development faces significant challenges, partly because a cell culture system to propagate human NoV was only recently established (21, 22). Consequently, much of what is known about human NoV biology has been inferred from other caliciviruses including FCV and murine norovirus (MNV) (23). Both viruses are easily cultured, and MNV in particular has been widely used to screen potential human NoV antivirals in cell culture and mouse models (24).

Other significant *Caliciviridae* pathogens include sapovirus (SaV), FCV, and RHDV. SaV infects a wide range of species including humans, swine and marine mammals (25), whilst RHDV is a highly contagious pathogen that has been used as an effective rabbit biocontrol agent (26). Together with benign rabbit calicivirus (RCV), RHDV is a member of the *Lagovirus* genus that infects the European rabbit, *Oryctolagus cuniculus* (27).

Non-nucleoside inhibitors (NNIs) are antivirals that bind to the RdRp allosterically, preventing polymerase conformational changes required for replication (28). All clinically approved NNIs to-date offer only narrow-spectrum, species-specific activity, developed against either HIV (29) or HCV (30). The HCV RdRp has five defined NNI binding sites (31) including: Thumb I (TI), Thumb II (TII), Palm I (PI), Palm II (PII) and Palm β (Pβ) (Figure 1A). Previously, we reported that HCV TI- and PII-binding NNIs exhibit cross-genotypic activity

against HCV (32), indicating the potential for a wider antiviral spectrum. To identify broad-spectrum calicivirus RdRp targets, we used HCV NNIs as an initial probe for inhibitory activity against the human NoV RdRp, and then against a range of caliciviral RdRps.

Whilst HCV NNI RdRp binding sites are well defined, much less is known about the human NoV RdRp. Currently only three human NoV NNI binding sites have been described, largely because few NoV NNIs have been reported (33). These three NoV RdRp NNI binding sites include one site across the fingers and thumb domains in the RdRp NTP access pathway (34, 35), and two binding sites in the thumb domain, named Site-A and Site-B (34).

Site-A is a positively charged cleft for NTP traversal, with flexible amino acid side chains (34). This flexibility poses challenges to structure-based antiviral development; therefore Site-A is less attractive than Site-B as an antiviral target site (34).

Co-crystallization studies of the human NoV RdRp and suramin were used to identify its binding pocket in the NTP access pathway between the fingers and thumb domains (35). Other examples of compounds that bind in each NNI site include suramin derivatives such as NF023 which binds the NTP access pathway (35); naphthalene di-sulfonate (NAF2) which binds in Site-A (34); and NAF2 and pyridoxal-5'-phosphate-6-(2'-naphthylazo-6'-nitro-4',8'-disulfonate) tetrasodium salt (PPNDS; Table 1) which both bind in Site-B (34).

However, suramin and its derivatives, including PPNDS, are poor drug candidates, demonstrating cell permeability issues due to the negative charges on the sulfonate groups (36, 37), thus limiting bioavailability and antiviral efficacy in viral culture (38). Additionally, PPNDS has been eliminated from other studies due to non-specific, off-target activities (39), and therefore it lacks the drug-like properties required for further antiviral development.

PPNDS was first reported as a potent P2X1 receptor agonist (40), but subsequently demonstrated potent inhibition of human NoV and MNV RdRps (34, 41) with IC_{50} values

between 0.45–0.88 μM (34, 41). Co-crystallization studies with the human NoV RdRp showed that PPNDS notably interacts with the Site-B amino acids Q414 and R419, amongst others (34). PPNDS reportedly inhibits transcription by fixing the C-terminal end of the RdRp within the active site, blocking the incoming RNA template and NTPs (34).

In this study, we aimed to identify broadly-active NNI scaffolds for further antiviral development. Representative HCV NNIs were used to probe calicivirus RdRps from the *Norovirus*, *Sapovirus* and *Lagovirus* genera for inhibition of transcription. We identified three HCV NNIs with pan-*Caliciviridae* activity. The second aim of this study was to identify highly-conserved domains across calicivirus RdRps, to target for *de novo* BS-AV development. Using *in silico* studies and site-directed mutagenesis we identified Site-B as a highly-conserved, broad-spectrum calicivirus RdRp pocket, which can now be targeted for antiviral development through *de novo* drug design.

2 Materials and Methods

2.1 Test compounds

Compounds (Table 1) were purchased from commercial vendors and dissolved in 100% dimethyl sulfoxide (DMSO). Compounds: JTK-109 (Dalton, Toronto, Canada), TMC-647055 and Beclabuvir (BMS-791325; Taizhou Crene Biotechnology, Zhejiang, China), Tegobuvir (GS-9190) and Nesbuvir (HCV-796; Chemexpress, Shanghai, China), Filibuvir (PF-00868554) and Setrobuvir (ANA-598; Acme Biosciences, Palo Alto, CA, USA), Lomibuvir (VX-222; Selleckchem, Houston, TX, USA), 2'-C-methylcytidine (2CMC; Sigma-Aldrich, St. Louis, MO, USA), 3'-deoxyguanosine-5'-triphosphate (3'dGTP; TriLink Biotechnologies, San Diego, CA, USA), PPNDS (Molport, Riga, Latvia).

2.2 Recombinant RdRp expression, purification and mutagenesis

Recombinant calicivirus RdRps (GenBank accession numbers) NoV GII.4 Den Haag 2006b (**EF684915**), NoV GII.4 Sydney 2012 (**KT239579**), MNV CW1 (**DQ285629**), RCV Australia 1 MIC-07, (**EU871528.1**), RHDV Czech V351 (**KF594473.1**), and SaV GI Mc114 (**AY237422**) were expressed and purified as described (42, 43). Mutant RdRps were generated using QuikChange site-directed mutagenesis kits (Agilent Technologies, Santa Clara, CA, USA), and confirmed by Sanger sequencing.

2.3 Quantitative RdRp activity and gel-based assays

Fluorescent activity assays were performed as described (33, 44). GraphPad Prism V6.05 (La Jolla, CA, USA) was used to plot the IC_{50} values. Primed elongation activity was examined as in (43), with an RNA template modified from (45), replacing six 5' ribonucleotides with 10 cytidines (PE44-NoV; Figure 3A). Antagonism was calculated using Compusyn software V1.0

(46). JTK-109 and PPNDS were tested alone and together (4:1 ratio) against NoV GII.4 Sydney 2012 RdRp.

2.4 Inhibition of MNV plaque formation in cell culture

MNV-1 (CW1) culture assays were performed as described (33). Replication was examined using plaque assays (47, 48). Cytotoxicity was examined using CellTitre Blue (Promega, Madison, WI, USA) viability assays (33).

2.5 *In silico* studies of the JTK-109 binding site

Molecular docking studies were performed on Viglen Genie Intel®CoreTM i7-3770 vPro CPU@ 3.40 GHz x 8 running Ubuntu 14.04 using Molecular Operating Environment (MOE) 2015.10 (49) and Maestro (Schrödinger Release 2016-1) (50) programs as described (51, 52). Briefly, a 12 Å docking grid was generated using the PPNDS structure (Site-B) as the centroid. The NoV RdRp crystal structure bound to PPNDS was downloaded from the Protein Data Bank (PDB) (53). Calicivirus RdRps (54) were aligned and superposed using the MOE2015.10 Protein Align/Superpose.

3 Results

3.1 HCV TI-binding NNI inhibits human NoV RdRp

Six HCV NNIs were selected to represent each of the five known HCV allosteric RdRp binding sites (**Error! Reference source not found.**A), including: JTK-109 (TI), Lomibuvir and Filibuvir (TII), Setrobuvir (PI), Nesbuvir (PII) and Tegobuvir (Pβ) (Table 1, Figure 1A). The inhibitory effects of each NNI (0.01 pM – 100 µM) were quantified against human NoV GII.4 RdRp (Den Haag 2006b) activity, using a fluorescence-based activity assay (44) (**Error! Reference source not found.**B). Of all the NNIs tested, only the HCV RdRp TI-binder JTK-109 demonstrated significant, dose-dependent inhibition of NoV RdRp activity, with an IC_{50} of 12.6 µM (**Error! Reference source not found.**B).

3.2 Pan-*Caliciviridae* antiviral activity of three HCV NNIs

NoV RdRp inhibition was observed with JTK-109, which binds in the HCV TI pocket (55). Therefore, JTK-109 and two other HCV TI-binders currently in clinical trials, namely TMC-647055 (56) and Beclabuvir (57), were selected for further assessment.

Using a quantitative fluorescent *de novo* RdRp assay (33), the synthesis of double-stranded RNA from an single-stranded RNA polycytidine template was monitored in the presence of the three HCV inhibitors (0.1–100 µM). Six RdRps spanning the *Norovirus*, *Lagovirus* and *Sapovirus* genera were tested: NoV GII.4 Sydney 2012, NoV GII.4 Den Haag 2006b, RCV, RHDV, MNV and SaV RdRps (**Error! Reference source not found.**; RdRp protein sequence identity range: 30.2–95.9%). All three HCV TI-binding NNIs demonstrated antiviral activity against the calicivirus RdRps. JTK-109 inhibited the six RdRps in a dose-dependent fashion, with IC_{50} values between 4.3 µM (NoV GII.4 Sydney 2012 RdRp) and 16.6 µM (SaV RdRp; **Error! Reference source not found.**, Table 2). TMC-647055 also inhibited the activity

of all six calicivirus RdRps (IC_{50} range: 18.8–45.4 μM; **Error! Reference source not found.**, Table 2), whilst Beclabuvir demonstrated modest inhibition of NoV and SaV RdRps (IC_{50} range: 23.8–92.6 μM), however, was ineffective against the MNV, RCV and RHDV RdRps (IC_{50} values >100 μM; **Error! Reference source not found.**, Table 2).

3.3 JTK-109 inhibits calicivirus RdRp primed elongation

As JTK-109 exhibited the most potent broad-spectrum inhibition in the *de novo* RdRp activity assays, it was examined for inhibition of primed-elongation activity using gel-shift assays (58). The RNA template [PE44-NoV; modified from (45)] allows primed transcription to extend the template from 32 to 44 nucleotides (Figure 3A). Elongation of PE44-NoV by the human NoV GII.4 Sydney 2012 RdRp was assessed in the presence of JTK-109 (0.1–100 μM) and the nucleoside analogue (NA) 3'dGTP (10 μM, Table 1) was used as a positive inhibition control (**Error! Reference source not found.**). In the absence of inhibitors (0.5% DMSO [vol/vol], vehicle only), the RNA template was extended, resulting in an upward gel shift (Figure 3). In the presence of JTK-109, the product formation was attenuated at 10 μM and almost completely abolished at 100 μM (**Error! Reference source not found.**A). This result is consistent with the fluorescence-based NoV RdRp assay results (IC_{50} 4.3 μM, Table 2). Similar results were obtained for human NoV GII.4 Den Haag 2006b, MNV, SaV, RCV and RHDV RdRps with JTK-109 in the gel-shift assay at a fixed concentration of 100 μM (Figure 3B).

3.4 JTK-109 inhibits MNV replication in cell culture

Plaque reduction assays were used to further examine the antiviral activity of JTK-109. RAW264.7 cell monolayers were infected with MNV and treated with JTK-109 (0.5–10.0 μM). JTK-109 inhibited MNV plaque formation in a dose-dependent manner, with an EC_{50} of 6.1 μM (95% CI: 5.1–7.3 μM, Figures 4A, 4D). The NA 2CMC (Table 1) was used as a positive

antiviral control, demonstrating complete inhibition of MNV plaque formation at 10.0 μM (Figure 4D). JTK-109 had no significant effect on RAW264.7 cell viability within the concentration range examined (0.5–10.0 μM; Figure 4B, Figure S1).

The effects of JTK-109 on MNV viral titers were also examined. JTK-109 concentrations ranged from 0.5–10.0 μM and were compared to the vehicle only (negative control). Viral titers (PFU/mL) were reduced by JTK-109 treatment (relative to mock) in a step-wise fashion (Figure 4C), consistent with the plaque reduction assays.

3.5 Identification of a BS-AV binding pocket

The RdRp thumb domain is a highly diverse region in terms of sequence and structure (59) between viral families. Therefore, whilst the TI binding pocket for JTK-109 on the HCV RdRp is well defined (60), it was uncertain whether it would bind to the same location in calicivirus RdRps. *In silico* studies using superimposition of the two RdRp crystal structures (53, 54, 61), revealed that the two alpha-helices present in the HCV RdRp, which form the TI domain, were not present in the NoV RdRp. Therefore, the equivalent HCV JTK-109 binding pocket appears to be absent in the human NoV polymerase, suggesting JTK-109 binds elsewhere. Moreover, molecular docking studies of JTK-109 in the corresponding region of the NoV RdRp also found no possible binding sites.

Further molecular docking of JTK-109 on the NoV GII.4 Sydney 2012 RdRp structure identified a potential binding site spanning two previously identified NNI binding sites (Site-A and Site-B; Figure 5A) (34). The predicted binding site revealed interactions between JTK-109 moieties and highly-conserved Site-B amino acids, particularly Q414 and R419.

To validate the docked model of the JTK-109 binding pocket, we generated two RdRps with mutations proposed to be critical for binding, Q414A and R419A, which are both located in the Site-B pocket. Transcriptional activity of the mutant RdRps was confirmed, then their

relative activity was examined in the presence of JTK-109 (0.1–100 μM; Figure 5B). These data supported the *in silico* study results, as both mutant RdRps were resistant to JTK-109, and neither reached 50% inhibition even at 100 μM, compared to an IC_{50} of 6.3 μM against the wildtype RdRp (Figure 5B).

Representative RdRp structures from the *Norovirus*, *Lagovirus* and *Sapovirus* genera were superimposed to reveal that Site-B is a highly-conserved RdRp pocket across the three caliciviral genera examined (Figure 5C). Additionally, protein alignments showed Q414 is conserved within all calicivirus RdRps examined, while R419 is conserved in the human NoV RdRps and is substituted for lysine, another basic amino acid, in all other calicivirus RdRps. These two mutations that confer resistance lie within the NoV RdRp thumb domain, but neither are located within the functional RdRp motifs, A–G (Figure 5D).

3.6 PPNDS is antagonistic with JTK-109 and has BS-AV activity against calicivirus RdRps

As the *in silico* and mutational studies revealed that JTK-109 binds within the RdRp Site-B, we predicted competitive antagonism between JTK-109 and other Site-B binding compounds such as PPNDS. Therefore, the inhibitory effects of JTK-109 (0.1–100 μM) and PPNDS (0.025–25 μM) were examined alone and together (4:1 ratio) against the transcriptional activity of the NoV GII.4 Sydney 2012 RdRp (Figure 6A). The average combination index of the NNIs at 50%, 75% and 90% inhibition was 3.1, confirming the two compounds were antagonistic (Figure 6A), indicating that both molecules bind to Site-B.

As Site-B is conserved within all calicivirus RdRps tested, PPNDS was examined for inhibitory activity against the six RdRps using a fluorescent activity assay (0.025–10 μM; Figure 6B). PPNDS was found to be a potent *in vitro* transcription inhibitor for all calicivirus RdRps (IC_{50} range: 0.1-2.3 μM, Figure 6B, Table 2). This was confirmed using a gel-shift assay with the human NoV GII.4 Sydney 2012 RdRp (0.01–10 μM; Figure 6C), and the RNA template PE44-

NoV (Figure 3A). PPNDS demonstrated dose-dependent inhibition, almost completely abrogating template extension activity at 10 μM. Similar results with PPNDS were obtained for human NoV GII.4 Den Haag 2006b, MNV, SaV, RCV and RHDV RdRps in the gel-shift assay at a fixed concentration of 10 μM (Figure 6D). However, PPNDS only demonstrated modest inhibition of MNV plaque formation in cell culture (20.5% inhibition at 10 μM, Figure 6E), demonstrating considerably less potency in cell-based assays compared to the *in vitro* fluorescence (IC_{50} value: 2.3 μM) and gel-based assays.

4 Discussion

Despite significant research efforts, there are currently no calicivirus-specific antivirals available (62). To reduce the global impact of caliciviruses, there is a demand to develop safe and effective antiviral therapies (63). BS-AVs are attractive therapeutics, offering the promise of a single antiviral to combat several viral pathogens.

The two major classes of antivirals used to target viral RdRps are NNIs and NAs, with NAs already in clinical use as BS-AVs [reviewed in (1)]. Unlike NNIs that bind allosterically, NAs mimic incoming NTPs and the RdRp erroneously incorporates them during transcription, causing chain termination (64) or lethal mutagenesis (65). This antiviral class includes ribavirin (66) which is used to treat several viral infections including respiratory syncytial virus (67) and HCV (68). Similarly, Favipiravir is an approved NA for treating influenza patients in Japan (69) and is also active against several RNA viruses in mouse models, including Ebola virus (70). In addition, 2CMC has been shown in preclinical studies to inhibit the replication of several viruses including human NoV (71) and MNV (72), as well as dengue virus, HCV, yellow fever virus and West Nile virus (73), amongst others. Moreover, 2CMC is probably the most promising and well-studied caliciviral antiviral, with moderate activity demonstrated in MNV cell culture (EC_{50} ~2 μM) (72), the NoV replicon (EC_{50} 18 μM) (74) and more recently, in a newly developed human NoV culture system (EC_{50} 0.3 μM) (75). However, development of 2CMC (Valopicitabine) for HCV treatment was halted following reports of undesirable gastrointestinal effects, suggesting its use for the treatment of other viruses such as human NoV, is unlikely.

The broad-spectrum antimicrobial compound, Nitazoxanide, has successfully treated a single NoV-infected patient (76). Despite reported antiviral activity *in vitro* against the NoV replicon (IC_{50} 1.6 μM), influenza viruses (IC_{50} range: 0.7 μM – 4.9 μM), HCV genotype 1 (IC_{50}

0.3 μM), and HBV (IC_{50} 0.2 μM), amongst other viruses (77), its mode of action is not yet understood and further studies are needed. These BS-AVs are largely in the early stages of development and currently no calicivirus-specific antivirals are available.

Numerous antivirals have been developed against HCV, and several FDA-approved direct-acting antivirals are now available (30). Therefore, repurposing HCV antivirals should be considered for the treatment of other viral infections, or for use in identifying valid antiviral targets.

In this study, we identified three NNIs that bind to the HCV TI pocket, JTK-109, TMC-647055 and Beclabuvir, which demonstrated dose-dependent RdRp inhibition across the three *Caliciviridae* genera examined. Additionally, JTK-109 exhibited dose-dependent inhibition of both primed elongation and *de novo* RNA synthesis, as well as a reduction of MNV plaque formation in cell culture, but demonstrated a low therapeutic index of 4.0.

There is minimal protein sequence similarity (less than 25%) between NoV and HCV RdRps, and the thumb domain is the most diverse region (59). Whilst the HCV RdRp features an elaborate thumb domain involved in *de novo* RNA synthesis, calicivirus RdRps use a protein-linked primer and template, thus requiring a wider template-binding channel (59). Therefore, calicivirus RdRp thumb domains are smaller and less complex than the equivalent HCV RdRp region, and there is no corresponding TI binding pocket present on the NoV RdRp. Given these differences, an *in silico* investigation was used to identify the potential JTK-109 binding pocket on the human NoV RdRp. Docking studies revealed that JTK-109 binds in the NoV thumb domain and predominantly interacts with Site-B, through the conserved amino acids Q414 and R419, which was supported by generating drug resistant mutants. Of interest, Site-B is the same binding site reported for NAF2 and PPNDS in the human NoV RdRp, and both amino acids Q414 and R419 were shown to be involved in their binding (34). PPNDS and

JTK-109 were antagonistic in combination, as expected for compounds that occupy the same binding site (Site-B) (34). Additionally, overlays of the calicivirus RdRp structures revealed that Site-B is highly-conserved within the *Caliciviridae*, and supporting this analysis, the Site-B binder PPNDS was a potent transcription inhibitor in all six calicivirus RdRps examined.

PPNDS has been reported as an inhibitor of *Norovirus* RdRp activity (34, 41), and this was supported in this study with additional observed inhibition of *Lagovirus* and *Sapovirus* RdRp transcriptional activities. However, PPNDS was relatively ineffective against MNV replication in cell culture. This discrepancy is likely due to its charged phosphate head that cannot pass through the cell membrane, which is reflected by the cell permeability issues observed with suramin (78) and its other derivatives. Moreover, PPNDS exhibits non-specific inhibitory effects (39), and therefore lacks the drug-like properties required for further medicinal development. In contrast, several HCV TI-binders have progressed through phase II and III clinical trials and could be further developed against other viruses using *in silico* drug design and structure-activity relationship chemistry to improve selectivity, cytotoxicity and potency profiles.

In conclusion, by probing caliciviral RdRps with HCV NNIs we identified three BS-AV scaffolds as potential platforms for calicivirus antiviral design. Secondly, we identified that the caliciviral RdRp Site-B is a highly-conserved, broad-spectrum target for *de novo* antiviral development.

Acknowledgments

We thank Dr Andrew Kelly (FairJourney Biologics), Dr Kun-Lee Lim (Singapore General Hospital) and Dr John-Sebastian Eden (University of Sydney) for advice and technical support.

Funding information

This work was partially funded by a National Health and Medical Research Council project grants (APP1083139 and APP1123135). NN, JL and DE acknowledge support through Australian Postgraduate Awards, and JL acknowledges additional support from a Water Research Australia Postgraduate Scholarship. NU acknowledges support from the Invasive Animals Cooperative Research Centre and a University of Canberra International Postgraduate Research Scholarship. SF and AB acknowledge support from the Life Science Research Network Wales grant no. NRNPGSep14008, an initiative funded through the Welsh Government's Ser Cymru program. The funding bodies had no role in the project design, data collection, analysis, interpretation, writing or decision to submit this article.

Conflicts of Interest

The authors declare no conflict of interest.

5 References

1. Debing Y, Neyts J, Delang L. The future of antivirals: broad-spectrum inhibitors. Curr Opin Infect Dis. 2015;28(6):596-602.
2. Martinez JP, Sasse F, Bronstrup M*, et al.* Antiviral drug discovery: broad-spectrum drugs from nature. Nat Prod Rep. 2015;32(1):29-48.
3. Gotte M, Feld JJ. Direct-acting antiviral agents for hepatitis C: structural and mechanistic insights. Nat Rev Gastroenterol Hepatol. 2016.
4. Murakami Y, Hayakawa M, Yano Y*, et al.* Discovering novel direct acting antiviral agents for HBV using in silico screening. Biochem Biophys Res Commun. 2015;456(1):20-8.
5. Cihlar T, Fordyce M. Current status and prospects of HIV treatment. Curr Opin Virol. 2016;18:50-6.
6. Warren TK, Wells J, Panchal RG*, et al.* Protection against filovirus diseases by a novel broad-spectrum nucleoside analogue BCX4430. Nature. 2014;508(7496):402-5.
7. Malet H, Masse N, Selisko B*, et al.* The flavivirus polymerase as a target for drug discovery. Antiviral Res. 2008;80(1):23-35.
8. Ng KK, Arnold JJ, Cameron CE. Structure-function relationships among RNA-dependent RNA polymerases. Curr Top Microbiol Immunol. 2008;320:137-56.

9. Ferrer-Orta C, Arias A, Escarmis C*, et al.* A comparison of viral RNA-dependent RNA polymerases. Curr Opin Struct Biol. 2006;16(1):27-34.
10. Gong EY, Kenens H, Ivens T*, et al.* Expression and purification of dengue virus NS5 polymerase and development of a high-throughput enzymatic assay for screening inhibitors of dengue polymerase. Antiviral Methods and Protocols. 2013:237-47.
11. Clarke IN, Estes, M.K., Green, K.Y., Hansman, G.S., Knowles, N.J., Koopmans, M.K., Matson, D.O., Meyers, G., Neill, J.D., Radford, A., Smith, A.W., Studdert, M.J., Thiel, H.-J. and Vinjé, J. Caliciviridae. San Diego; 2012 2012. Report No.: 9th Report
12. Clarke IN, Lambden PR. The molecular biology of caliciviruses. J Gen Virol. 1997;78 (Pt 2):291-301.
13. van Asten L, Siebenga J, van den Wijngaard C*, et al.* Unspecified gastroenteritis illness and deaths in the elderly associated with norovirus epidemics. Epidemiology. 2011;22(3):336-43.
14. Lee LE, Cebelinski EA, Fuller C*, et al.* Sapovirus outbreaks in long-term care facilities, Oregon and Minnesota, USA, 2002-2009. Emerg Infect Dis. 2012;18(5):873-6.
15. Delibes-Mateos M, Ferreira C, Carro F*, et al.* Ecosystem effects of variant rabbit hemorrhagic disease virus, Iberian Peninsula. Emerg Infect Dis. 2014;20(12):2166-8.
16. Radford AD, Dawson S, Coyne KP*, et al.* The challenge for the next generation of feline calicivirus vaccines. Vet Microbiol. 2006;117(1):14-8.
17. Abrantes J, van der Loo W, Le Pendu J*, et al.* Rabbit haemorrhagic disease (RHD) and rabbit haemorrhagic disease virus (RHDV): a review. Vet Res. 2012;43:12.
18. Koo HL, Ajami N, Atmar RL*, et al.* Noroviruses: The leading cause of gastroenteritis worldwide. Discov Med. 2010;10(50):61-70.
19. Ahmed SM, Hall AJ, Robinson AE*, et al.* Global prevalence of norovirus in cases of gastroenteritis: a systematic review and meta-analysis. Lancet Infect Dis. 2014;14(8):725-30.
20. Bartsch SM, Lopman BA, Ozawa S*, et al.* Global Economic Burden of Norovirus Gastroenteritis. PLoS One. 2016;11(4):e0151219.
21. Jones MK, Watanabe M, Zhu S*, et al.* Enteric bacteria promote human and mouse norovirus infection of B cells. Science. 2014;346(6210):755-9.
22. Ettayebi K, Crawford SE, Murakami K*, et al.* Replication of human noroviruses in stem cell-derived human enteroids. Science. 2016;353(6306):1387-93.
23. Karst SM, Wobus CE, Lay M*, et al.* STAT1-dependent innate immunity to a Norwalk-like virus. Science. 2003;299(5612):1575-8.
24. Wobus CE, Thackray LB, Virgin HWt. Murine norovirus: a model system to study norovirus biology and pathogenesis. J Virol. 2006;80(11):5104-12.
25. Tse H, Chan WM, Li KS*, et al.* Discovery and genomic characterization of a novel bat sapovirus with unusual genomic features and phylogenetic position. PLoS One. 2012;7(4):e34987.
26. Green KY, Ando T, Balayan MS*, et al.* Taxonomy of the caliciviruses. J Infect Dis. 2000;181 Suppl 2:S322-30.
27. Capucci L, Fusi P, Lavazza A*, et al.* Detection and preliminary characterization of a new rabbit calicivirus related to rabbit hemorrhagic disease virus but nonpathogenic. J Virol. 1996;70(12):8614-23.
28. Caillet-Saguy C, Simister PC, Bressanelli S. An objective assessment of conformational variability in complexes of hepatitis C virus polymerase with non-nucleoside inhibitors. J Mol Biol. 2011;414(3):370-84.
29. US Food and Drug Administration. FDA approves Viekira Pak to treat hepatitis C: U.S. Food and Drug Administration; 2014 [updated December 19, 2014. Available from: http://www.fda.gov/NewsEvents/Newsroom/PressAnnouncements/ucm427530.htm.
30. Hepatitis C Support Project. Drug pipeline – quick reference guides; 2016 [cited 2016 June]. Available from: http://hcvadvocate.org/treatment/drug-pipeline/.
31. Eltahla AA, Luciani F, White PA*, et al.* Inhibitors of the Hepatitis C Virus Polymerase; Mode of Action and Resistance. Viruses. 2015;7(10):5206-24.

32. Eltahla AA, Tay E, Douglas MW*, et al.* Cross-genotypic examination of hepatitis C virus polymerase inhibitors reveals a novel mechanism of action for thumb binders. Antimicrob Agents Chemother. 2014;58(12):7215-24.
33. Eltahla AA, Lim KL, Eden JS*, et al.* Nonnucleoside inhibitors of norovirus RNA polymerase: scaffolds for rational drug design. Antimicrob Agents Chemother. 2014;58(6):3115-23.
34. Tarantino D, Pezzullo M, Mastrangelo E*, et al.* Naphthalene-sulfonate inhibitors of human norovirus RNA-dependent RNA-polymerase. Antiviral Res. 2014;102:23-8.
35. Mastrangelo E, Pezzullo M, Tarantino D*, et al.* Structure-based inhibition of Norovirus RNA-dependent RNA polymerases. J Mol Biol. 2012;419(3-4):198-210.
36. Beindl W, Mitterauer T, Hohenegger M*, et al.* Inhibition of receptor/G protein coupling by suramin analogues. Mol Pharmacol. 1996;50(2):415-23.
37. Klinger M, Bofill-Cardona E, Mayer B*, et al.* Suramin and the suramin analogue NF307 discriminate among calmodulin-binding sites. Biochem J. 2001;355(Pt 3):827-33.
38. Croci R, Pezzullo M, Tarantino D*, et al.* Structural bases of norovirus RNA dependent RNA polymerase inhibition by novel suramin-related compounds. PLoS One. 2014;9(3):e91765.
39. Simeonov A, Kulkarni A, Dorjsuren D*, et al.* Identification and characterization of inhibitors of human apurinic/apyrimidinic endonuclease APE1. PLoS One. 2009;4(6):e5740.
40. Lambrecht G, Rettinger J, Baumert HG*, et al.* The novel pyridoxal-5'-phosphate derivative PPNDS potently antagonizes activation of P2X(1) receptors. Eur J Pharmacol. 2000;387(3):R19-21.
41. Croci R, Tarantino D, Milani M*, et al.* PPNDS inhibits murine Norovirus RNA-dependent RNA-polymerase mimicking two RNA stacking bases. FEBS Lett. 2014;588(9):1720-5.
42. Bull RA, Eden JS, Rawlinson WD*, et al.* Rapid evolution of pandemic noroviruses of the GII.4 lineage. PLoS Pathog. 2010;6(3):e1000831.
43. Urakova N, Netzler N, Kelly AG*, et al.* Purification and Biochemical Characterisation of Rabbit Calicivirus RNA-Dependent RNA Polymerases and Identification of Non-Nucleoside Inhibitors. Viruses. 2016;8(4).
44. Eltahla AA, Lackovic K, Marquis C*, et al.* A fluorescence-based high-throughput screen to identify small compound inhibitors of the genotype 3a hepatitis C virus RNA polymerase. J Biomol Screen. 2013;18(9):1027-34.
45. Campagnola G, Gong P, Peersen OB. High-throughput screening identification of poliovirus RNA-dependent RNA polymerase inhibitors. Antiviral Res. 2011;91(3):241-51.
46. Chou TC. Drug combination studies and their synergy quantification using the Chou-Talalay method. Cancer Res. 2010;70(2):440-6.
47. Rocha-Pereira J, Cunha R, Pinto DC*, et al.* (E)-2-styrylchromones as potential anti-norovirus agents. Bioorg Med Chem. 2010;18(12):4195-201.
48. Schneider CA, Rasband WS, Eliceiri KW. NIH Image to ImageJ: 25 years of image analysis. Nat methods. 2012;9(7):671-5.
49. Chemical Computing Group I. Molecular Operating Environment (MOE 2015.10) Montreal, Quebec, Canada: Chemical Computing Group, Inc.; 2015 [Available from: http://www.chemcomp.com.
50. Schrödinger Release 2016-1: Maestro [Internet]. Schrödinger. 2016 [cited 25 March, 2017].
51. Grande F, Parisi OI, Mordocco RA*, et al.* Quercetin derivatives as novel antihypertensive agents: Synthesis and physiological characterization. Eur J Pharm Sci. 2016;82:161-70.
52. Bassetto M, Leyssen P, Neyts J*, et al.* Computer-aided identification, synthesis and evaluation of substituted thienopyrimidines as novel inhibitors of HCV replication. Eur J Med Chem. 2016;123:31-47.
53. RCSB. PDB code 4LQ3 2013 [Available from: http://www.rcsb.org/pdb/explore/explore.do?structureId=4LQ3.
54. RCSB. PDB codes 4O4R, 5TFR, 2CKW, 2J7U, 2J7W, 2BRK: Protein Data Bank; 2013 [Available from: http://www.rcsb.org/pdb/home/home.do.
55. Hirashima S, Suzuki T, Ishida T*, et al.* Benzimidazole derivatives bearing substituted biphenyls as hepatitis C virus NS5B RNA-dependent RNA polymerase inhibitors: structure-activity relationship

studies and identification of a potent and highly selective inhibitor JTK-109. J Med Chem. 2006;49(15):4721-36.
56. Devogelaere B, Berke JM, Vijgen L*, et al.* TMC647055, a potent nonnucleoside hepatitis C virus NS5B polymerase inhibitor with cross-genotypic coverage. Antimicrob Agents Chemother. 2012;56(9):4676-84.
57. Gentles RG, Ding M, Bender JA*, et al.* Discovery and preclinical characterization of the cyclopropylindolobenzazepine BMS-791325, a potent allosteric inhibitor of the hepatitis C virus NS5B polymerase. J Med Chem. 2014;57(5):1855-79.
58. Yi G, Deval J, Fan B*, et al.* Biochemical study of the comparative inhibition of hepatitis C virus RNA polymerase by VX-222 and filibuvir. Antimicrob Agents Chemother. 2012;56(2):830-7.
59. Choi KH, Groarke JM, Young DC*, et al.* The structure of the RNA-dependent RNA polymerase from bovine viral diarrhea virus establishes the role of GTP in de novo initiation. Proc Natl Acad Sci U S A. 2004;101(13):4425-30.
60. Kukolj G, McGibbon GA, McKercher G*, et al.* Binding site characterization and resistance to a class of non-nucleoside inhibitors of the hepatitis C virus NS5B polymerase. J Biol Chem. 2005;280(47):39260-7.
61. Elhefnawi M, ElGamacy M, Fares M. Multiple virtual screening approaches for finding new hepatitis C virus RNA-dependent RNA polymerase inhibitors: structure-based screens and molecular dynamics for the pursue of new poly pharmacological inhibitors. BMC Bioinformatics. 2012;13 Suppl 17:S5.
62. Rocha-Pereira J, Neyts J, Jochmans D. Norovirus: targets and tools in antiviral drug discovery. Biochem Pharmacol. 2014;91(1):1-11.
63. Rohayem J, Bergmann M, Gebhardt J*, et al.* Antiviral strategies to control calicivirus infections. Antiviral Res. 2010;87(2):162-78.
64. Galmarini CM, Mackey JR, Dumontet C. Nucleoside analogues: mechanisms of drug resistance and reversal strategies. Leukemia. 2001;15(6):875-90.
65. Loeb LA, Essigmann JM, Kazazi F*, et al.* Lethal mutagenesis of HIV with mutagenic nucleoside analogs. Proc Natl Acad Sci U S A. 1999;96(4):1492-7.
66. Smith RA, Kirkpatrick W. Ribavirin: a broad spectrum antiviral agent: Academic Press, Inc., 1ll Fifth Avenue, New York, NY 10003, USA; 1980.
67. Marcelin JR, Wilson JW, Razonable RR*, et al.* Oral ribavirin therapy for respiratory syncytial virus infections in moderately to severely immunocompromised patients. Transpl Infect Dis. 2014;16(2):242-50.
68. Reichard O, Yun ZB, Sonnerborg A*, et al.* Hepatitis C viral RNA titers in serum prior to, during, and after oral treatment with ribavirin for chronic hepatitis C. J Med Virol. 1993;41(2):99-102.
69. Kiso M, Takahashi K, Sakai-Tagawa Y*, et al.* T-705 (favipiravir) activity against lethal H5N1 influenza A viruses. Proc Natl Acad Sci U S A. 2010;107(2):882-7.
70. Oestereich L, Ludtke A, Wurr S*, et al.* Successful treatment of advanced Ebola virus infection with T-705 (favipiravir) in a small animal model. Antiviral Res. 2014;105:17-21.
71. Kolawole AO, Rocha-Pereira J, Elftman MD*, et al.* Inhibition of human norovirus by a viral polymerase inhibitor in the B cell culture system and in the mouse model. Antiviral Res. 2016.
72. Rocha-Pereira J, Jochmans D, Dallmeier K*, et al.* Inhibition of norovirus replication by the nucleoside analogue 2'-C-methylcytidine. Biochem Biophys Res Commun. 2012;427(4):796-800.
73. Pierra C, Amador A, Benzaria S*, et al.* Synthesis and pharmacokinetics of valopicitabine (NM283), an efficient prodrug of the potent anti-HCV agent 2'-C-methylcytidine. J Med Chem. 2006;49(22):6614-20.
74. Jin Z, Tucker K, Lin X*, et al.* Biochemical Evaluation of the Inhibition Properties of Favipiravir and 2'-C-Methyl-Cytidine Triphosphates against Human and Mouse Norovirus RNA Polymerases. Antimicrob Agents Chemother. 2015;59(12):7504-16.
75. Kolawole AO, Rocha-Pereira J, Elftman MD*, et al.* Inhibition of human norovirus by a viral polymerase inhibitor in the B cell culture system and in the mouse model. Antiviral Res. 2016;132:46-9.

76. Siddiq DM, Koo HL, Adachi JA*, et al.* Norovirus gastroenteritis successfully treated with nitazoxanide. J Infect. 2011;63(5):394-7.
77. Rossignol JF. Nitazoxanide: a first-in-class broad-spectrum antiviral agent. Antiviral Res. 2014;110:94-103.
78. Mastrangelo E, Mazzitelli S, Fabbri J*, et al.* Delivery of suramin as an antiviral agent through liposomal systems. ChemMedChem. 2014;9(5):933-9.
79. Chan L, Das SK, Reddy TJ*, et al.* Discovery of thiophene-2-carboxylic acids as potent inhibitors of HCV NS5B polymerase and HCV subgenomic RNA replication. Part 1: Sulfonamides. Bioorg Med Chem Lett. 2004;14(3):793-6.
80. Li H, Tatlock J, Linton A*, et al.* Discovery of (R)-6-cyclopentyl-6-(2-(2,6-diethylpyridin-4-yl)ethyl)-3-((5,7-dimethyl-[1,2,4]tr iazolo[1,5-a]pyrimidin-2-yl)methyl)-4-hydroxy-5,6-dihydropyran-2-one (PF-00868554) as a potent and orally available hepatitis C virus polymerase inhibitor. J Med Chem. 2009;52(5):1255-8.
81. Shih IH, Vliegen I, Peng B*, et al.* Mechanistic characterization of GS-9190 (Tegobuvir), a novel nonnucleoside inhibitor of hepatitis C virus NS5B polymerase. Antimicrob Agents Chemother. 2011;55(9):4196-203.
82. Gopalsamy A, Chopra R, Lim K*, et al.* Discovery of proline sulfonamides as potent and selective hepatitis C virus NS5b polymerase inhibitors. Evidence for a new NS5b polymerase binding site. J Med Chem. 2006;49(11):3052-5.
83. Kneteman NM, Howe AY, Gao T*, et al.* HCV796: A selective nonstructural protein 5B polymerase inhibitor with potent anti-hepatitis C virus activity in vitro, in mice with chimeric human livers, and in humans infected with hepatitis C virus. Hepatology. 2009;49(3):745-52.
84. Heck JA, Lam AM, Narayanan N*, et al.* Effects of mutagenic and chain-terminating nucleotide analogs on enzymes isolated from hepatitis C virus strains of various genotypes. Antimicrob Agents Chemother. 2008;52(6):1901-11.

Tables

Table 1. Antiviral compounds used in this study.

Compound	Structure	Molecular weight (g/mol)	Inhibitor class	Original target	HCV RdRp binding site	Reference
JTK-109	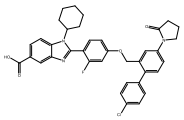	638.1	NNI	HCV	TI	(55)
TMC-647055	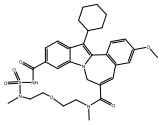	606.7	NNI	HCV	TI	(56)
Beclabuvir (BMS-791325)	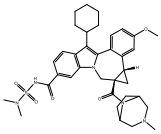	659.8	NNI	HCV	TI	(57)
Lomibuvir (VX-222)	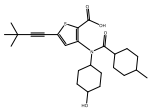	445.6	NNI	HCV	TII	(79)
Filibuvir (PF868554)	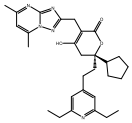	503.6	NNI	HCV	TII	(80)
Tegobuvir (GS-9190)	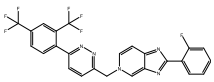	517.4	NNI	HCV	Pβ	(81)
Setrobuvir (ANA-598)	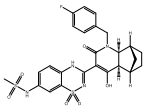	560.6	NNI	HCV	PI	(82)
Nesbuvir (HCV-796)	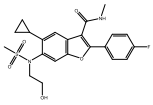	446.5	NNI	HCV	PII	(83)
PPNDS	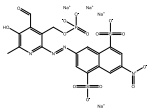	694.3	NNI	NoV	N/A	(34)
2'-C-Methylcytidine* (2CMC)	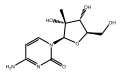	257.2	NA	HCV	N/A	(72)
3'-deoxyguanosine-5'-triphosphate* (3'dGTP)	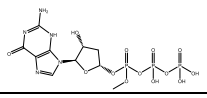	507.2	NA	HCV / pestiviruses	N/A	(84)

* Assay control compounds

Table 2. Broad-spectrum activities of NNIs against calicivirus polymerases.

Virus	Family	Genus	Genotype	Strain	NNI IC_{50}[a] [µM] *in vitro* RdRp assay (95% CI[b])			
					JTK-109	TMC-647055	Beclabuvir	PPNDS
NoV	*Caliciviridae*	*Norovirus*	GII.4	Sydney 2012	4.3 (2.2-8.5)	28.3 (22.7-35.3)	23.8 (20.7-27.3)	1.4 (1.2-1.7)
NoV	*Caliciviridae*	*Norovirus*	GII.4	Den Haag 2006b	10.2 (9.0-11.7)	18.8 (12.7-27.7)	92.6 (41.0-209.6)	0.8 (0.6-1.0)
MNV	*Caliciviridae*	*Norovirus*	GIV.1	MNV CW1	10.9 (7.5-15.8)	23.2 (15.0-35.8)	>100	2.3 (1.8-4.3)
RHDV	*Caliciviridae*	*Lagovirus*	ND	Czech V-351	7.6 (5.9-9.9)	45.4 (39.4-52.4)	>100	0.6 (0.5-0.7)
RCV	*Caliciviridae*	*Lagovirus*	ND	Australia 1 MIC-07	15.0 (12.4-18.1)	36.5 (27.8-48.0)	>100	1.3 (1.0-1.7)
SaV	*Caliciviridae*	*Sapovirus*	GI	Mc114	16.6 (11.7-23.6)	37.6 (29.7-47.7)	48.6 (44.2-53.4)	0.1 (0.1-0.3)
HCV	*Flaviviridae*	*Hepacivirus*	G1b	Con1 / BK	0.02[c]	0.03[d]	0.004[e]	N/D

Grey shading denotes results published previously, outside of this study.

[a] IC_{50}: half maximal inhibitory concentration determined by *in vitro* RdRp assays

[b] CI: confidence interval

[c] IC_{50} with HCV genotype 1b BK RdRp (55)

[d] IC_{50} with HCV genotype 1b, Con1 RdRp (56)

[e] IC_{50} with HCV genotype 1b, Con1 RdRp (57)

Figure Legends

Fig. 1. Probing the human NoV RdRp for cross-inhibitory activity with HCV NNIs. A) The HCV RdRp domains are color-coded on the ribbon diagram: fingers (red), palm (green), thumb (blue) and palm b (yellow). HCV NNI binding sites are shown in colored circles, adapted from (Eltahla et al., 2015). B) Inhibitory effects of six HCV NNIs on human NoV GII.4 Den Haag 2006b RdRp activity were examined using a fluorescence-based RdRp transcription assay. NNIs (0.01-100 µM) were compared to samples containing the compound

vehicle only (0.5% DMSO [vol/vol]). Mean values from triplicate technical replicates are plotted with standard deviations.

Fig. 2. HCV TI-binding NNIs inhibit calicivirus RdRp activity. The inhibitory effects of three HCV TI-binding NNIs were examined on the transcriptional activity of six recombinant calicivirus RdRps. The dose-response effects were analysed by monitoring the formation of double-stranded RNA from the single-stranded RNA homopolymeric cytidine template, using a fluorescent RdRp assay. Compound concentrations ranged between 0.1 and 100 µM and RdRp activity was compared to the relative activity of mock treated samples (vehicle only). The six panels above include the following RdRps: A) NoV GII.4 Sydney 2012, B) NoV GII.4 Den Haag 2006b, C) MNV, D) RCV, E) RHDV and F) SaV. The mean values from triplicate datasets from three independent experiments are plotted with standard deviations. The half maximal inhibitory concentration (IC_{50}) values for each NNI with the six calicivirus RdRps are shown on the graph and in Table 2.

Fig. 3. JTK-109 inhibits calicivirus RdRp primed elongation. A) The effects of JTK-109 on human NoV GII.4 Sydney 2012 RdRp primed elongation activity were examined using a gel shift assay. PE44-NoV RNA templates (32 nucleotides) were extended (44 nucleotides) by the RdRp without JTK-109 (vehicle only) or with JTK-109 (concentration range: 0.1-100 µM). The nucleoside analogue 3'dGTP is used as a positive control (10 µM; Table 1) and no RdRp is used as a negative control. B) JTK-109 is assessed at a fixed concentration of 100 µM and compared to the effect of DMSO (vehicle only) against human NoV GII.4 Den Haag 2006b, MNV, SaV, RCV and RHDV RdRps. Human NoV GII.4 Sydney 2012 is used as a positive assay control with 3'dGTP as the inhibition control (10 µM) to demonstrate total inhibition.

Fig. 4. JTK-109 inhibits MNV replication in cell culture. Inhibition of MNV plaque formation and viral titers was examined using a plaque reduction assay in RAW264.7 cell monolayers. A) Total plaque area (mm2) is compared between JTK-109 treated cells (0.5-10 μM) and mock treated samples (vehicle only). B) JTK-109 has no effect on cell viability at concentrations up to 10 μM. C) MNV titers (PFU/mL) are reduced by JTK-109 (0.5-10 μM) in a step-wise fashion. Mean values of triplicate technical replicates are plotted with standard deviations. D) Plaque area reduction assay results (for panel A) are shown (triplicate datasets: black underline), with positive control (2CMC, 10 μM), negative control (vehicle only) and JTK-109 (0.5-10 μM).

Fig. 5. Identification of a broad-spectrum NNI binding pocket. A) *In silico* studies of the JTK-109 binding site on human NoV GII.4 Sydney 2012 RdRp (using PDB-ID: 4LQ3). RdRp domains are color-coded: fingers (red), palm (green), thumb (blue). JTK-109 (cyan structure) binds across Site-A (red shadow) and Site-B RdRp (blue shadow). Interacting amino acids are color-coded: Q414 (grey sticks, green dotted shadow), R419 (grey sticks, purple dotted shadow). B) Relative inhibitory effects of JTK-109 on wildtype NoV GII.4 Sydney 2012 RdRp activity (blue), compared to mutants Q414A (green) and R419A (purple). The hashed red line indicates 50% inhibition compared to mock treated samples (vehicle only) and IC_{50} values are shown on the graph. The mean values of triplicate datasets are shown from three independent experiments. C) Superimposition of calicivirus RdRp structures from Norovirus (blue, PDB-ID: 4LQ3), Lagovirus (cyan, PDB-ID: 1KHW), Sapovirus (yellow, PDB-ID: 2CKW) with conserved interacting JTK-109 regions labelled: Q414, R/K419. D) Schematic of human NoV RdRp structural domains are color-coded: fingers (red), palm (green), thumb (blue), with functional motifs A-G indicated. Asterisks in the thumb domain indicate

JTK-109 resistance mutations: Q414A (green) and R419A (purple).

Fig. 6. Antagonism of Site-B binders and pan-Caliciviridae activity of PPNDS. A) Isobologram of JTK-109 (0.1-100 μM) and PPNDS (0.025-10 μM) examined in a 4:1 ratio respectively. Together both molecules demonstrate antagonism against human NoV GII.4 Sydney 2012 RdRp activity with an average combination index of 3.1 over 50%, 75% and 90% inhibition. B) Inhibitory effects of PPNDS (0.025-10 μM) on calicivirus RdRp activities compared to mock treated samples (vehicle only). Mean values from triplicate technical replicates are plotted with standard deviations. IC_{50} values are shown on the graph and in Table 2. C) The effects of PPNDS on human NoV GII.4 Sydney 2012 RdRp primed elongation activity were examined using a gel shift assay. PE44-NoV (Fig. 3) RNA templates (32 nucleotides) were extended (44 nucleotides) by the RdRp without PPNDS (vehicle only) or with PPNDS (0.01-10 μM). The nucleoside analogue 3'dGTP is used as a positive control (10 μM; Table 1) and no RdRp (template only) was used as a negative control. D) PPNDS inhibition of caliciviral RdRp primed elongation activity was assessed at a fixed concentration of 10 μM and compared to the effect of DMSO (vehicle only) against human NoV GII.4 Den Haag 2006b, MNV, SaV, RCV and RHDV RdRps. Human NoV GII.4 Sydney 2012 is used as a positive assay control with 3'dGTP as the inhibition control (10 μM) to demonstrate total inhibition. E) The effects of PPNDS on MNV in cell culture were examined using a plaque reduction assay. Total plaque area (mm2) is compared in the presence of PPNDS (0.1-10 μM) to the vehicle only (negative control) and the nucleoside analogue (2CMC, 10 μM, positive control).

Figure S1. The effects of JTK-109 on RAW264.7 cell viability. Cell cytotoxicity of JTK-109 was measured with a metabolic resazurin-to-resorufin conversion assay. The percentages of

viable cells are shown in the presence of JTK-109 (0.1–100 μM) compared to mock control wells containing the compound vehicle only, DMSO (0.5% [vol/vol]). The half maximal cytotoxic concentration (CC_{50}) of JTK-109 on RAW264.7 cells was 24.7 μM (95% CI: 23.4–26.1 μM). The mean values of triplicate technical replicates are plotted with standard deviations.

Broad-spectrum non-nucleoside inhibitors for caliciviruses

Natalie E. Netzler [a], Daniel Enosi Tuipulotu [a,] Auda A. Eltahla [a,b], Jennifer H. Lun[a], Salvatore Ferla [c], Andrea Brancale [c], Nadya Urakova [d,e,f], Michael Frese [d,e,f,g], Tanja Strive [d,f,g], Jason M. Mackenzie [h,i] and Peter A. White [a#].

[a] *School of Biotechnology and Biomolecular Sciences, University of New South Wales, Sydney, NSW, Australia*

[b] *School of Medical Sciences, Faculty of Medicine, University of New South Wales, Sydney, NSW, Australia*

[c] *School of Pharmacy and Pharmaceutical Sciences, Cardiff University, Cardiff, United Kingdom*

[d] *CSIRO Health and Biosecurity, Canberra, ACT, Australia*

[e] *Invasive Animals Cooperative Research Centre, University of Canberra, ACT, Australia*

[f] *Health Research Institute, University of Canberra, ACT, Australia*

[g] *Institute for Applied Ecology, University of Canberra, ACT, Australia*

[h] *Department of Microbiology and Immunology, School of Biomedical Sciences, University of Melbourne, VIC, Australia*

[i] *The Peter Doherty Institute for Infection and Immunity, VIC, Australia.*

Highlights

(<6 plain language summary points, <125 chars)

- The *Caliciviridae* comprise several highly diverse human and non-human pathogens.
- Broad-spectrum antivirals could offer a significant advantage to rapidly combat multiple viral infections.
- A family of allosteric antivirals developed against hepatitis C virus also inhibited calicivirus replication.
- These antivirals are scaffolds for medicinal enhancement to improve potency, specificity and cytotoxicity profiles.
- The calicivirus polymerase binding site reveals a highly-conserved target for broad-spectrum antiviral development.

Figure 1

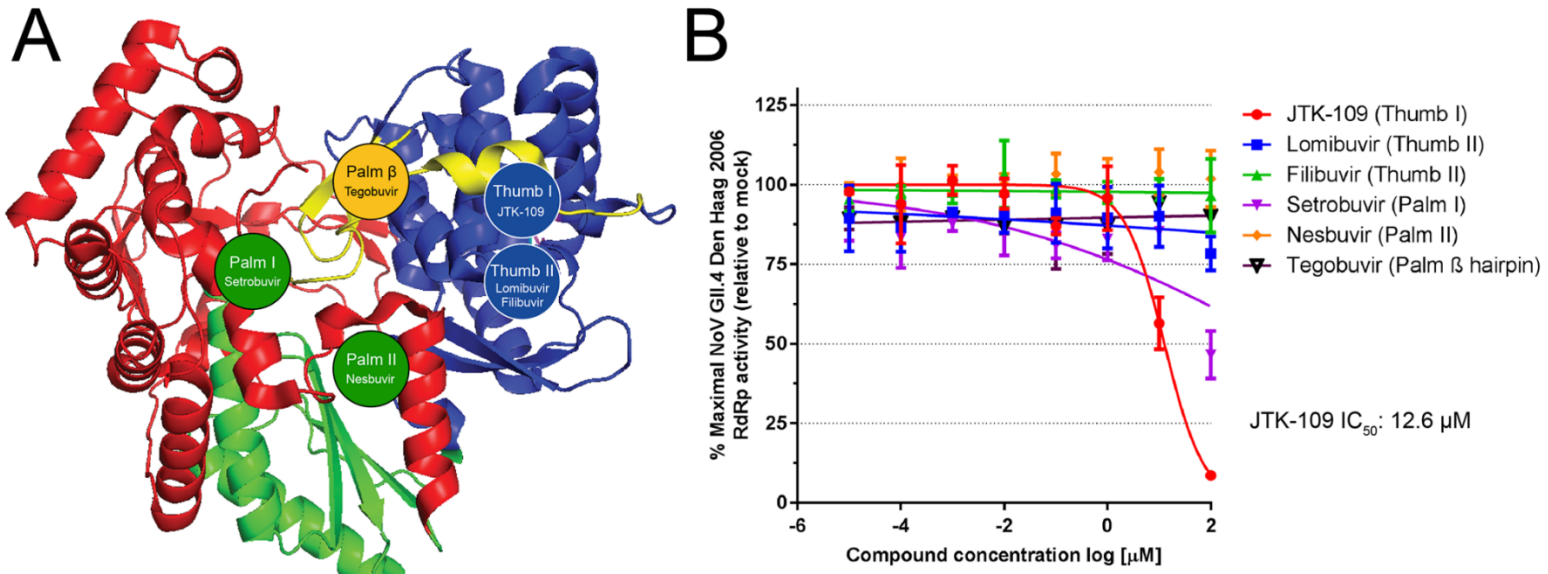
A
Palm β
Tegobuvir
Thumb I
JTK-109
Palm I
Setrobuvir
Thumb II
Lomibuvir
Filibuvir
Palm II
Nesbuvir
B
% Maximal NoV GII.4 Den Haag 2006 RdRp activity (relative to mock)
125
100
75
50
25
0
-6
-4
-2
0
2
Compound concentration log [µM]
JTK-109 (Thumb I)
Lomibuvir (Thumb II)
Filibuvir (Thumb II)
Setrobuvir (Palm I)
Nesbuvir (Palm II)
Tegobuvir (Palm ß hairpin)
JTK-109 IC50: 12.6 µM

Figure 2

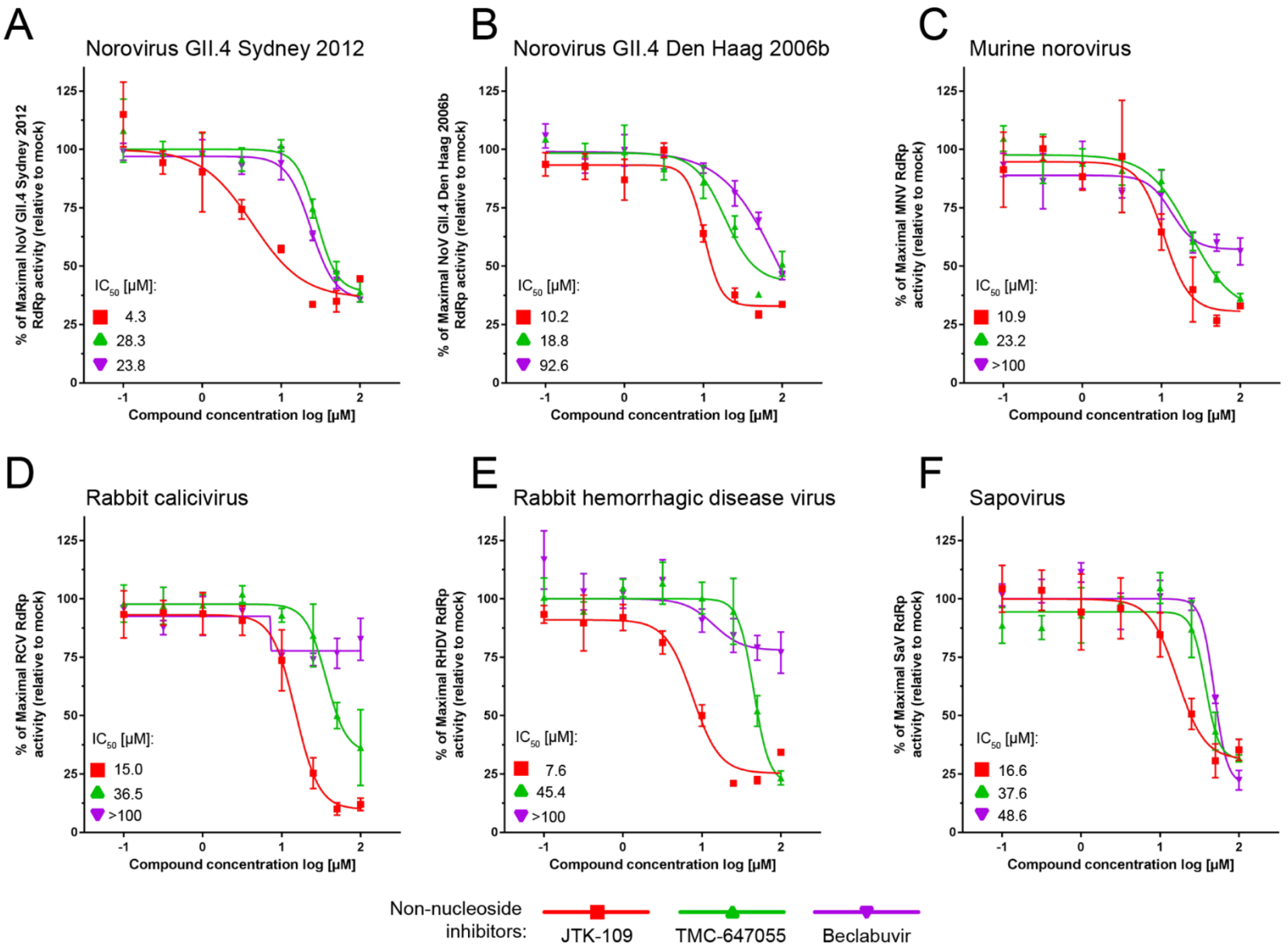
A
Norovirus GII.4 Sydney 2012
% of Maximal NoV GII.4 Sydney 2012 RdRp activity (relative to mock)
IC50 [µM]:
4.3
28.3
23.8
Compound concentration log [µM]
B
Norovirus GII.4 Den Haag 2006b
% of Maximal NoV GII.4 Den Haag 2006b RdRp activity (relative to mock)
IC50 [µM]:
10.2
18.8
92.6
Compound concentration log [µM]
C
Murine norovirus
% of Maximal MNV RdRp activity (relative to mock)
IC50 [µM]:
10.9
23.2
>100
Compound concentration log [µM]
D
Rabbit calicivirus
% of Maximal RCV RdRp activity (relative to mock)
IC50 [µM]:
15.0
36.5
>100
Compound concentration log [µM]
E
Rabbit hemorrhagic disease virus
% of Maximal RHDV RdRp activity (relative to mock)
IC50 [µM]:
7.6
45.4
>100
Compound concentration log [µM]
F
Sapovirus
% of Maximal SaV RdRp activity (relative to mock)
IC50 [µM]:
16.6
37.6
48.6
Compound concentration log [µM]
Non-nucleoside inhibitors:
JTK-109
TMC-647055
Beclabuvir

Figure 3

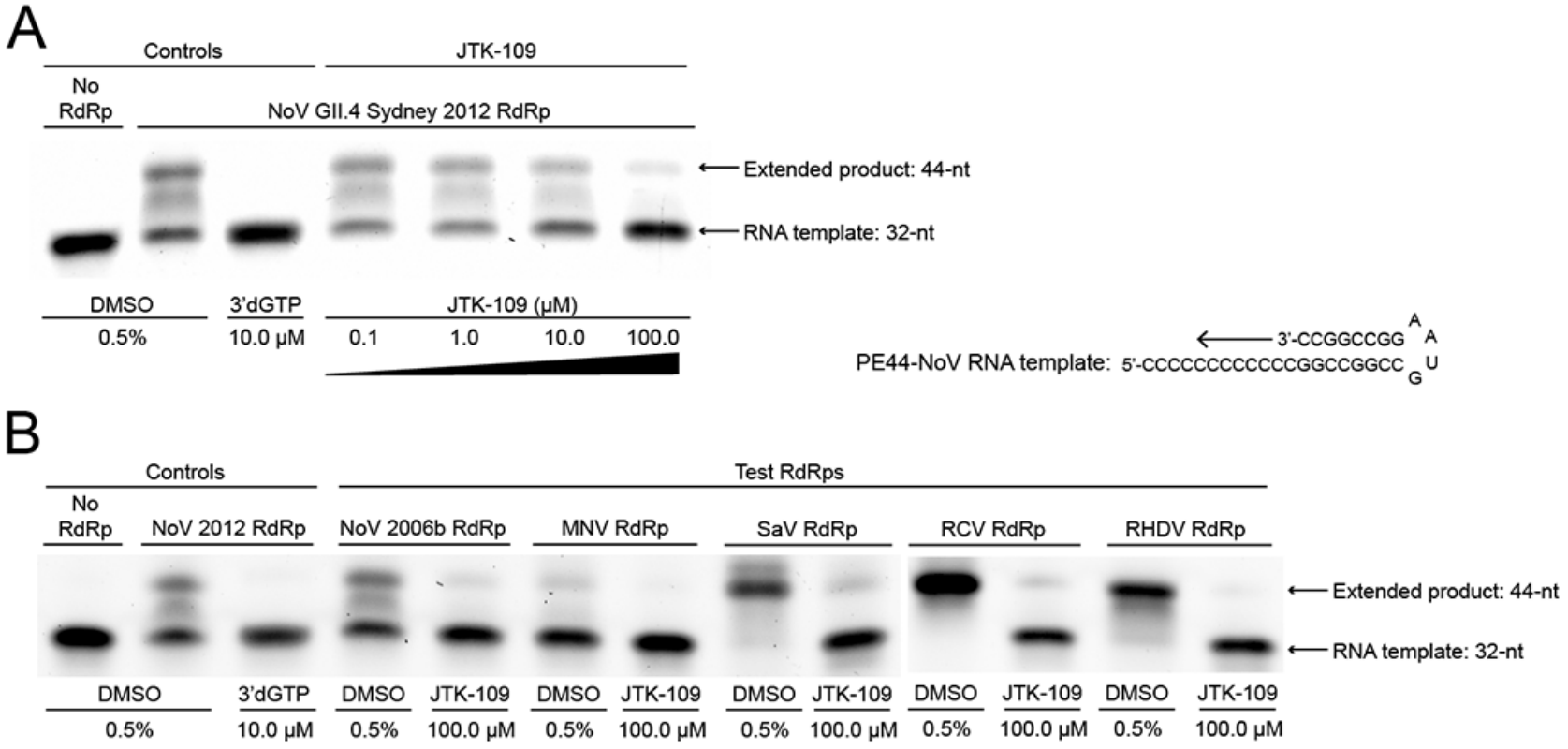
A
Controls
JTK-109
No RdRp
NoV GII.4 Sydney 2012 RdRp
Extended product: 44-nt
RNA template: 32-nt
DMSO
0.5%
3'dGTP
10.0 μM
JTK-109 (μM)
0.1
1.0
10.0
100.0
PE44-NoV RNA template:
3'-CCGGCCGG
5'-CCCCCCCCCCCCGGCCGGCC
B
Controls
Test RdRps
No RdRp
NoV 2012 RdRp
NoV 2006b RdRp
MNV RdRp
SaV RdRp
RCV RdRp
RHDV RdRp
Extended product: 44-nt
RNA template: 32-nt
DMSO
3'dGTP
JTK-109
0.5%
10.0 μM
100.0 μM

Figure 4

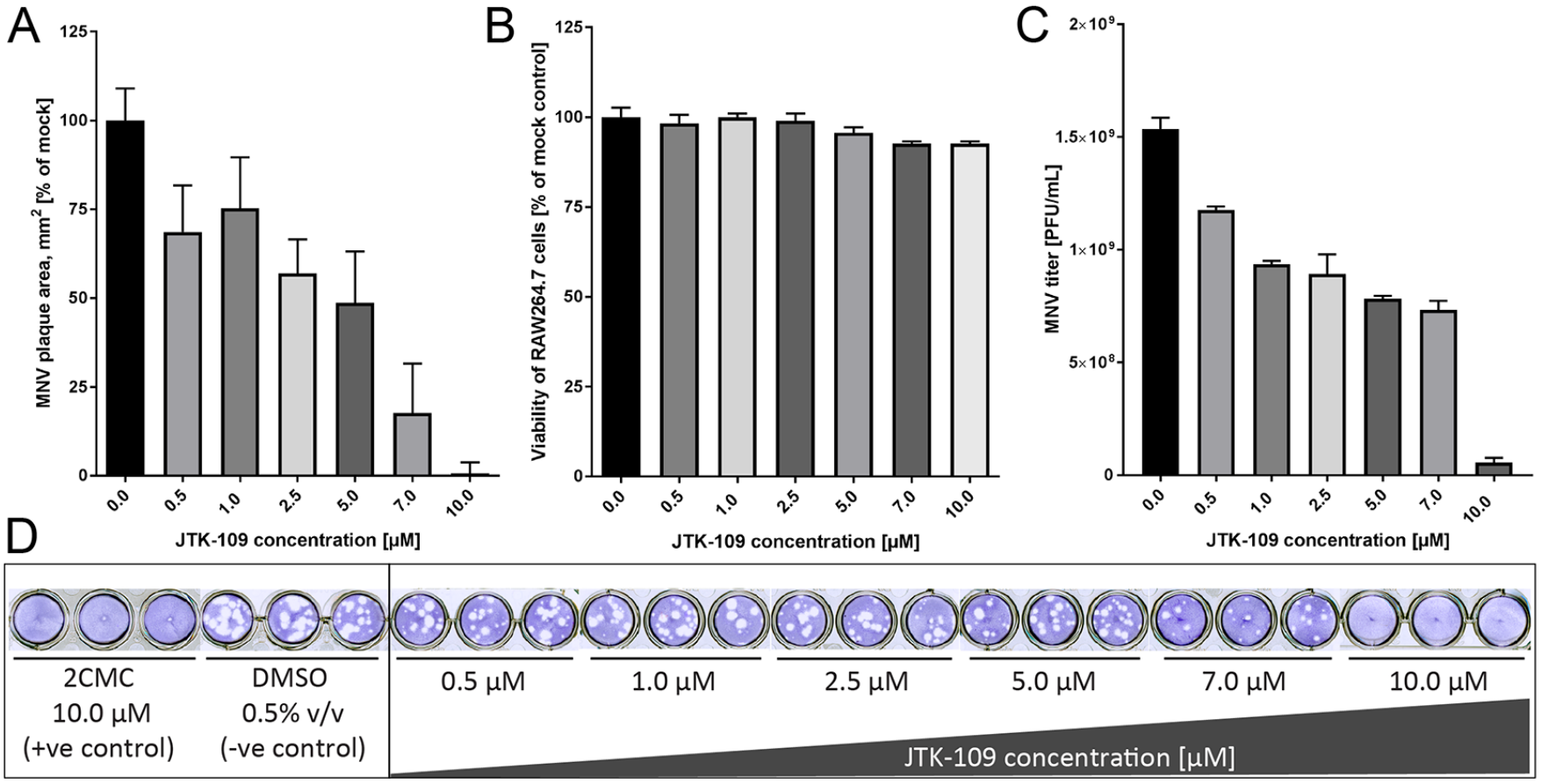
A
MNV plaque area, mm² [% of mock]
125
100
75
50
25
0
0.0
0.5
1.0
2.5
5.0
7.0
10.0
JTK-109 concentration [μM]
B
Viability of RAW264.7 cells [% of mock control]
125
100
75
50
25
0
0.0
0.5
1.0
2.5
5.0
7.0
10.0
JTK-109 concentration [μM]
C
MNV titer [PFU/mL]
2×10⁹
1.5×10⁹
1×10⁹
5×10⁸
0
0.0
0.5
1.0
2.5
5.0
7.0
10.0
JTK-109 concentration [μM]
D
2CMC
10.0 μM
(+ve control)
DMSO
0.5% v/v
(-ve control)
0.5 μM
1.0 μM
2.5 μM
5.0 μM
7.0 μM
10.0 μM
JTK-109 concentration [μM]

Figure 5

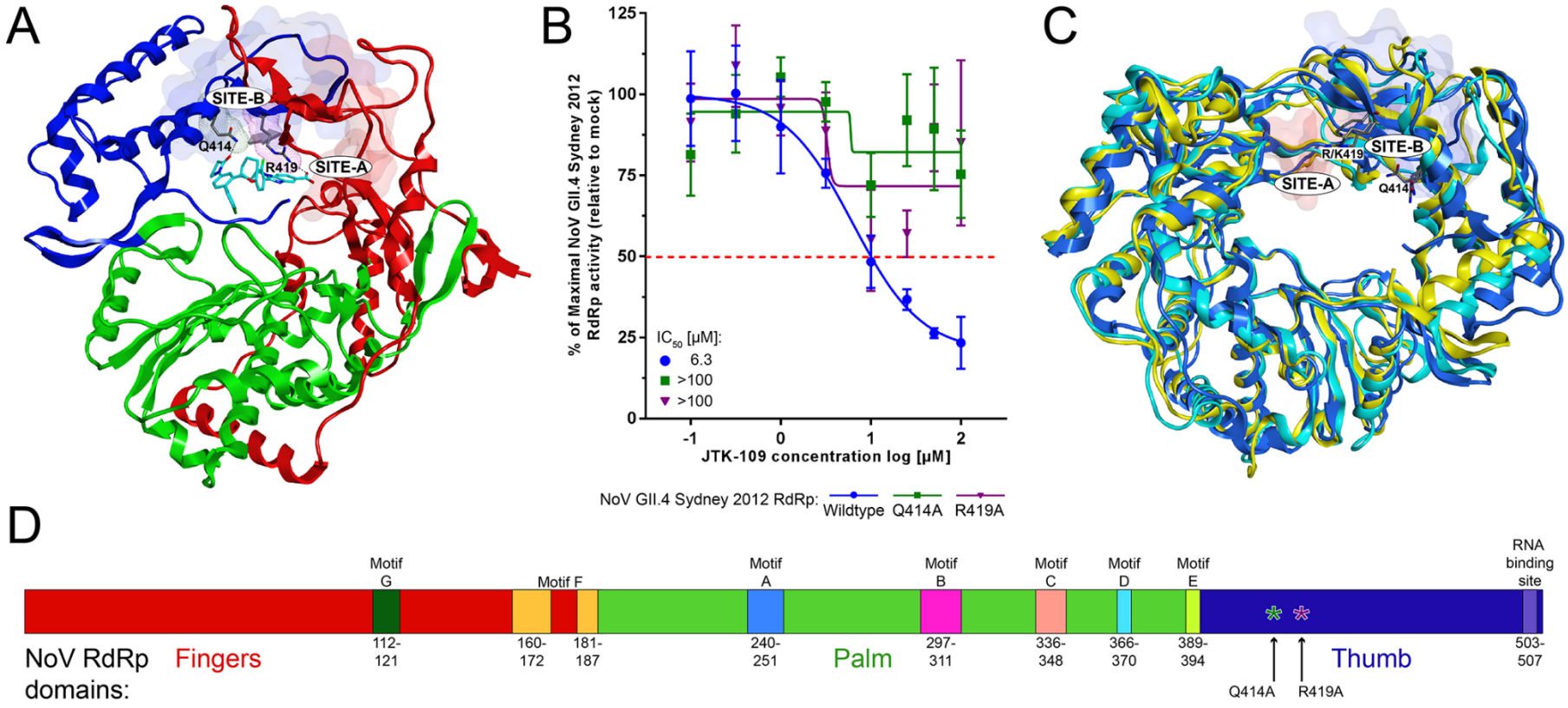
A
SITE-B
Q414
R419
SITE-A
B
% of Maximal NoV GII.4 Sydney 2012 RdRp activity (relative to mock)
125
100
75
50
25
0
IC50 [μM]:
6.3
>100
>100
-1
0
1
2
JTK-109 concentration log [μM]
NoV GII.4 Sydney 2012 RdRp:
Wildtype
Q414A
R419A
C
R/K419
SITE-B
SITE-A
Q414
D
Motif G
Motif F
Motif A
Motif B
Motif C
Motif D
Motif E
RNA binding site
NoV RdRp domains:
Fingers
Palm
Thumb
112-121
160-172
181-187
240-251
297-311
336-348
366-370
389-394
503-507
Q414A
R419A

Figure 6

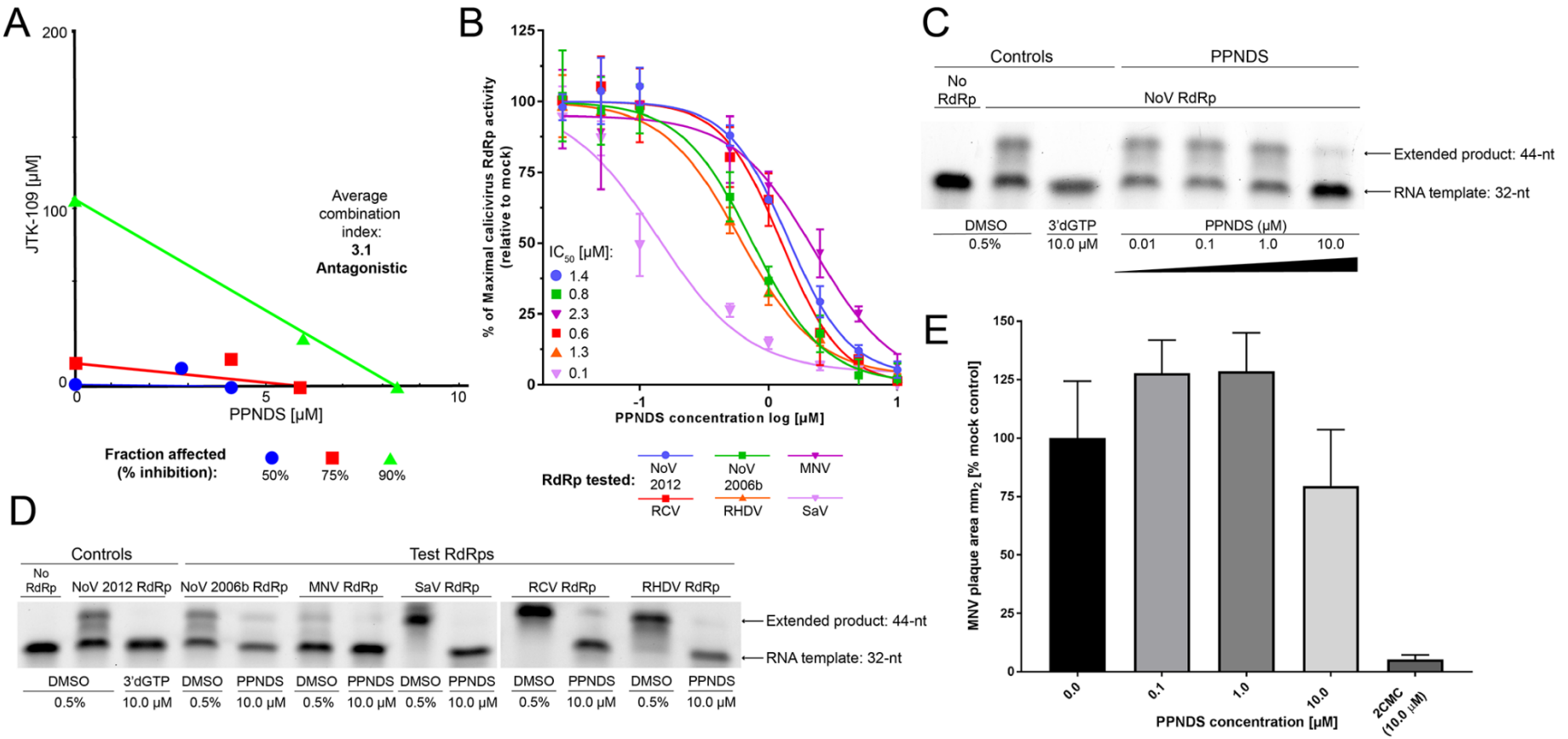
A
JTK-109 [μM]
PPNDS [μM]
Average combination index: 3.1 Antagonistic
Fraction affected (% inhibition):
50%
75%
90%
B
% of Maximal calicivirus RdRp activity (relative to mock)
PPNDS concentration log [μM]
IC50 [μM]:
1.4
0.8
2.3
0.6
1.3
0.1
RdRp tested:
NoV 2012
NoV 2006b
MNV
RCV
RHDV
SaV
C
Controls
PPNDS
No RdRp
NoV RdRp
Extended product: 44-nt
RNA template: 32-nt
DMSO 0.5%
3'dGTP 10.0 μM
PPNDS (μM)
0.01
0.1
1.0
10.0
D
Controls
Test RdRps
No RdRp
NoV 2012 RdRp
NoV 2006b RdRp
MNV RdRp
SaV RdRp
RCV RdRp
RHDV RdRp
Extended product: 44-nt
RNA template: 32-nt
DMSO 0.5%
3'dGTP 10.0 μM
PPNDS 10.0 μM
E
MNV plaque area mm2 [% mock control]
PPNDS concentration [μM]
2CMC (10.0 μM)

Table 1. Antiviral compounds used in this study.

Compound	Structure	Molecular weight (g/mol)	Inhibitor class	Original target	HCV RdRp binding site	Reference
JTK-109	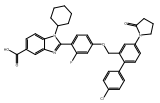	638.1	NNI	HCV	TI	(55)
TMC-647055	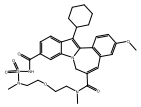	606.7	NNI	HCV	TI	(56)
Beclabuvir (BMS-791325)	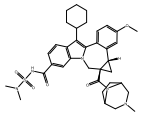	659.8	NNI	HCV	TI	(57)
Lomibuvir (VX-222)	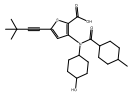	445.6	NNI	HCV	TII	(79)
Filibuvir (PF868554)	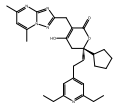	503.6	NNI	HCV	TII	(80)
Tegobuvir (GS-9190)	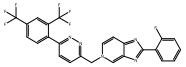	517.4	NNI	HCV	Pβ	(81)
Setrobuvir (ANA-598)	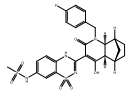	560.6	NNI	HCV	PI	(82)
Nesbuvir (HCV-796)	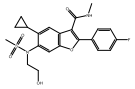	446.5	NNI	HCV	PII	(83)
PPNDS	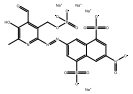	694.3	NNI	NoV	N/A	(34)
2'-C-Methylcytidine* (2CMC)	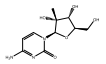	257.2	NA	HCV	N/A	(72)
3'-deoxyguanosine-5'-triphosphate* (3'dGTP)	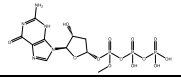	507.2	NA	HCV / pestiviruses	N/A	(84)

* Assay control compounds

Table 2. Broad-spectrum activities of NNIs against calicivirus polymerases *in vitro*.

Virus	Family	Genus	Genotype	Strain	NNI IC_{50}[a] [μM] *in vitro* RdRp assay (95% CI[b])			
					JTK-109	**TMC-647055**	**Beclabuvir**	**PPNDS**
NoV	*Caliciviridae*	*Norovirus*	GII.4	Sydney 2012	4.3 (2.2-8.5)	28.3 (22.7-35.3)	23.8 (20.7-27.3)	1.4 (1.2-1.7)
NoV	*Caliciviridae*	*Norovirus*	GII.4	Den Haag 2006b	10.2 (9.0-11.7)	18.8 (12.7-27.7)	92.6 (41.0-209.6)	0.8 (0.6-1.0)
MNV	*Caliciviridae*	*Norovirus*	GIV.1	MNV CW1	10.9 (7.5-15.8)	23.2 (15.0-35.8)	>100	2.3 (1.8-4.3)
RHDV	*Caliciviridae*	*Lagovirus*	ND	Czech V-351	7.6 (5.9-9.9)	45.4 (39.4-52.4)	>100	0.6 (0.5-0.7)
RCV	*Caliciviridae*	*Lagovirus*	ND	Australia 1 MIC-07	15.0 (12.4-18.1)	36.5 (27.8-48.0)	>100	1.3 (1.0-1.7)
SaV	*Caliciviridae*	*Sapovirus*	GI	Mc114	16.6 (11.7-23.6)	37.6 (29.7-47.7)	48.6 (44.2-53.4)	0.1 (0.1-0.3)
HCV	*Flaviviridae*	*Hepacivirus*	G1b	Con1 / BK	0.02[c]	0.03[d]	0.004[e]	N/D

Grey shading denotes results published previously, outside of this study.

[a] IC_{50}: half maximal inhibitory concentration determined by *in vitro* RdRp assays

[b] CI: confidence interval

[c] IC_{50} with HCV genotype 1b BK RdRp (55)

[d] IC_{50} with HCV genotype 1b, Con1 RdRp (56)

[e] IC_{50} with HCV genotype 1b, Con1 RdRp (57)

Figure S1

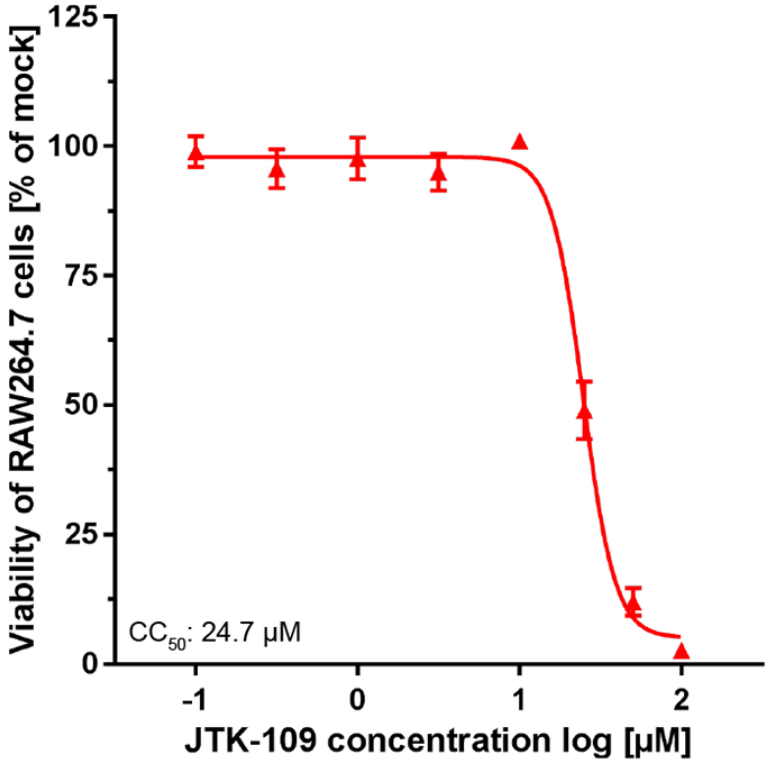
Viability of RAW264.7 cells [% of mock]
125
100
75
50
25
0
CC50: 24.7 μM
-1
0
1
2
JTK-109 concentration log [μM]